Materials and Structures/Matériaux et Constructions, Vol. **31**, November 1998, pp 628-633

SCIENTIFIC REPORTS

Behaviour of ferrocement confined reinforced concrete (FCRC) under axial compression

D.R Seshu [1] *and A.K Rao* [2]

(1) *Asst. Prof., Department of Civil Engineering,*

(2) *Prof., Regional Engineering College, Warangal-506 004, AP, India.*

Paper received: April 15, 1997; Paper accepted: September 22, 1997

ABSTRACT

An experimental investigation on the behaviour of ferrocement confined reinforced concrete (FCRC) under axial compression, by varying the specific surface factor (S_f) which controls the behaviour of ferrocement, is presented. A total of 270 prisms of size 150 × 150 × 300 mm were tested. The results indicated that additional confinement in the form of ferrocement shell improved the ultimate strength, strain at ultimate strength and the ductility of concrete. The improvement is in proportion to the S_f of the ferrocement shell for a given confinement index (C_i) of the lateral reinforcement

RÉSUMÉ

Une investigation expérimentale sur le comportement du béton armé d'un ferro-ciment confiné soumis à une compression axiale, par le biais d'une variation du facteur de surface spécifique (S_f), facteur qui sert à maîtriser le comportement du ferro-ciment, est présentée. Un total de 270 prismes d'une dimension de 150 × 150 × 300 mm a été testé. Les résultats démontrent qu'un confinement supplémentaire de la structure en ferro-ciment améliore la résistance ultime, la déformation à la résistance ultime et la ductilité du béton. L'amélioration ainsi obtenue est proportionnelle à la valeur S_f de la structure en ferro-ciment pour un indice de confinement (C_i) de l'armature latérale donnée.

NOTATIONS

b,d =	Lateral dimensions of prism
f_y =	Yield strength of longitudinal tie/mesh steel (Table 1)
A_s =	Area of longitudinal steel
f'_c =	Strength of unconfined concrete
ε'_c =	Strain at ultimate of unconfined concrete
f_{cb} =	Strength of tie confined concrete [7] $= (1+0.55\ C_i)\ f'_c$
ε_{cb} =	Strain at ultimate of tie confined concrete $= (1+5.2\ C_i)\ \varepsilon'_c$
Ag =	Gross cross-sectional area
K_t and K_f =	Coefficients as explained in the paper
C_i =	Confinement index
P_b =	Ratio of the volume of transverse steel to the volume of concrete
P_{bb} =	Ratio of volume of the transverse steel to the volume of concrete corresponding to a limiting pitch equal to 1.5b
f_v =	Stress in the lateral ties
s =	Spacing of ties
ε_{cf} =	Strain at ultimate of FCRC
$\varepsilon_{0.85cf}$ =	Strain at 85% of ultimate of FCRC in the descending portion of the stress-strain curve
f_{cf} =	Ultimate strength of FCRC

1. INTRODUCTION

The necessity of confining concrete by providing closely spaced rectangular stirrups to ensure adequate rotational capacity of reinforced concrete sections is now well established [9]. The improved rotational capacity obtained by confinement of critical sections of a structure will allow a better redistribution of moments, thus simplifying the limit state analysis of indeterminate structures. Further, this improved rotational capacity will give rise to better performance of the structure during earthquakes, blasts and settlement of foundations [1, 4, 5].

A review of the existing literature [4, 5] has shown that it is necessary to provide additional confinement to critical sections in a statically indeterminate structure along with the lateral stirrup (tie) confinement. In addition, it has also been indicated [2, 3, 10] that the provision of a ferrocement shell to a concrete core in an axially loaded compression member provides an effective confinement; such concrete has been termed 'Ferrocement Confined Reinforced Concrete' (FCRC). However, most of the conclusions reached in the earlier investigations are of a qualitative nature [2, 10]. In practice, the ferrocement shell cannot be provided without ties in columns or without stirrups in beams. In fact it will be wrapped around the cage of ties or stirrups.

In the present investigation a study [8] of the confining effect of the ferrocement shell, provided in addition to rectangular stirrups on concrete, is made in order to quantify the improvement in strength and failure strain of FCRC.

2. EXPERIMENTAL PROGRAMME

2.1 Scheme of experimental work

The experimental programme was designed to study the behaviour of concrete confined by the ferrocement shell under axial compression by testing prisms of size 150 mm × 150 mm × 300 mm. The variable in the study was the Specific Surface Factor (S_f), which controls the behaviour of ferrocement [6]. The specific surface factor is the product of the specific surface ratio and the yield stress of mesh wires in the direction of the force divided by the strength of plain mortar. The specific surface ratio is the ratio of the total surface area of contact of reinforcement wires present per unit length of the specimen in the direction of the application of load in a given width and thickness of the ferrocement shell to the volume of mortar.

The programme consisted of casting and testing 270 prisms, which were cast in 15 batches. The prisms in each batch were divided into 6 sets. In each set three identical specimens were cast and tested, and the average behaviour was taken to represent the behaviour for that set of three specimens. Hence, in each batch the total number of prisms amounted to 18. Out of the 6 sets, the first set consisted of plain concrete prisms, and the second set consisted of reinforced concrete prisms without any ferrocement shell as an additional confinement. In the remaining four sets, the reinforced concrete prisms with ferrocement shell as an additional confinement (FCRC) were cast, and in all these sets the amount of reinforcement (longitudinal steel and lateral ties) was maintained constant and equal to that provided in the prisms of the second set, but the amount of ferrocement shell confinement was varied by varying the S_f. Since the effect of confinement on concrete due to lateral reinforcement is already known [7], the effect of confinement due to the ferrocement shell can be separated. Each set was designated by the diameter of the lateral tie, the type of mesh and the number of layers of the wire mesh. Thus the designation 6A3 stands for a 6 mm diameter lateral tie, an 'A' type of mesh with 3 as the number of mesh layers. For plain concrete specimens, the number of mesh layers is replaced with the letter 'P'. The details of prisms tested are given in Table 1.

2.2 Materials used

The galvanised woven wire mesh of a square grid fabric was used in the ferrocement. The ties and longitudinal steel used in the prisms were made of mild steel. The cement used was OPC of 43 grade conforming to IS 8112-1981. Machine crushed hard granite chips passing through a 12.5-mm IS sieve and retained on a 4.75 mm IS sieve were used as coarse aggregate throughout the work. River sand procured locally was used as fine aggregate for the ferrocement shell; fine aggregate passing a 1.18 mm IS sieve was used. For the concrete core, fine aggregate passing a 2.36 mm IS sieve was used. In half the number of prisms, the core concrete used in the study was M15 grade and in the remaining half, M20 grade. The mortar used for the ferrocement shell has the mix proportion of one part cement and two parts sand (*i.e.* 1:2) with a water/cement ratio of 0.6.

2.3 Preparation of specimen

After the fabrication of reinforcement cages using ties and longitudinal steel, a sufficient number of wire mesh layers to provide the required S_f were wrapped over the ties tightly. The mesh was stitched thrice so as not to fail by splitting of the mesh. Fig. 1(a) shows the reinforcement details of the specimen. Fig. 1(b) shows the mould used for casting the prisms.

Table 1 – Details of prisms

Sl. No.	Specimen Designation	Longitudinal Reinforcement		Lateral Reinforcement		Mesh Reinforcement			f_c'	ε_c'
		Dia. (mm)	f_y (MPa)	Dia. (mm)	f_y (MPa)	Dia. (mm)	Spacing (mm)	f_y (MPa)	(MPa)	(10^{-6})
1.	6A0 - 6A4	3.2	387.5	5.6	222.0	0.390	2.20	300.0	16.0	1910
2.	6B0 - 6B4	3.2	387.5	5.6	222.0	0.490	4.50	290.0	21.5	2220
3.	6D0 - 6D4	3.2	387.5	5.6	222.0	0.540	3.03	270.0	17.5	2040
4.	6D0 - 6D4	5.6	222.0	5.6	222.0	0.370	2.27	310.0	15.0	2210
5.	6E0 - 6E4	5.6	222.0	5.6	222.0	0.580	4.35	275.0	17.0	2100
6.	6F0 - 6F4	5.6	222.0	5.6	222.0	0.720	7.14	250.0	17.0	2010
7.	6G0 - 6G4	5.6	222.0	5.6	222.0	0.580	4.61	367.5	12.1	2340
8.	6H0 - 6H4	5.6	222.0	5.6	222.0	0.465	3.81	275.0	14.9	2210
9.	6J0 - 6J4	5.6	222.0	5.6	222.0	0.390	2.02	314.0	13.3	1840
10.	8D0 - 8D4	5.6	292.5	8.7	292.5	0.370	2.27	310.0	16.0	2010
11.	8E0 - 8E4	5.6	292.5	8.7	292.5	0.580	4.35	275.0	18.0	2410
12.	8F0 - 8F4	5.6	292.5	8.7	292.5	0.720	7.14	250.0	20.0	2220
13.	8G0 - 8G4	5.6	292.5	8.7	292.5	0.580	4.61	367.5	12.8	2290
14.	8H0 - 8H4	5.6	292.5	8.7	292.5	0.465	3.81	275.0	15.0	2210
15.	8J0 - 8J4	5.6	292.5	8.7	292.5	0.390	2.02	314.0	14.8	2390

2.4 Casting of specimens

The prepared cage of reinforcement was kept in the moulds carefully. Spacer rods of 2 mm diameter galvanised iron wires were kept temporarily in between the layers of mesh to maintain spacing between the layers. The prisms were cast in the vertical position. First, the gap between the mould and the reinforcement was filled to about half the height of the mould using cement mortar, and then concrete was placed inside the mesh up to the same level. Then, a needle vibrator was

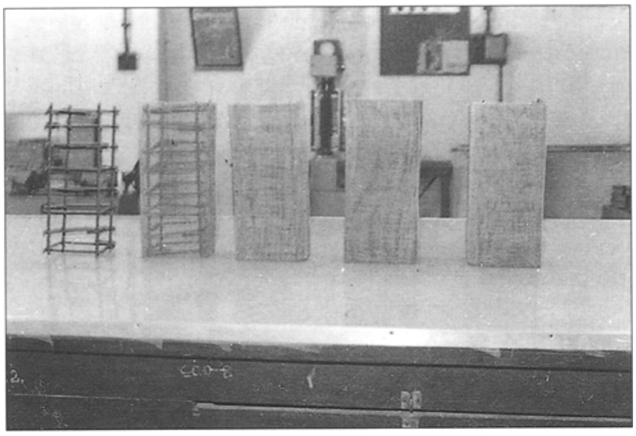

Fig. 1(a) – Reinforcement details in prisms.

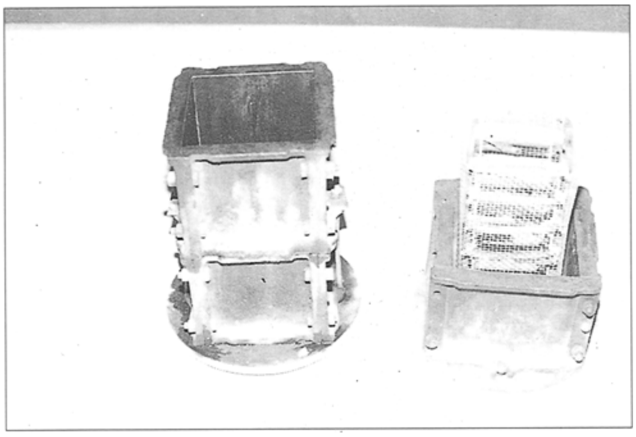

Fig. 1(b) – Mould used for casting the prisms.

used to compact the core concrete. The mould was filled in three layers using the same technique. The top face of the prism specimens was capped with a rich cement paste. The specimens was demoulded 48 hours after casting and cured for 28 days in the curing pond.

2.5 Testing

The cured specimens were capped with plaster of Paris before testing, to provide a smooth loading surface. A Tinius - Olsen testing machine of 1810 kN capacity was used for testing the prisms under axial compression. From the studies of previous investigators [5, 7] who worked on concrete confined with ties, it was observed that the cover concrete started spalling off at about 90 percent of the ultimate load. Along the concrete, the resistance strain gauges and Demec points fixed to the concrete surface usually came off. Also, the compressometer designed to measure the strains in standard concrete cylinders could not be fitted to the square prisms.

To overcome the above mentioned difficulties, compressometers suitable for prisms, which were fabricated by the earlier investigators [5, 7] on confined concrete, were adopted. Each compressometer consisted of two square frames, a top frame and a bottom frame made of 12 mm square mild steel bars. Each frame was attached to the concrete specimen by two diametrically opposite pairs of

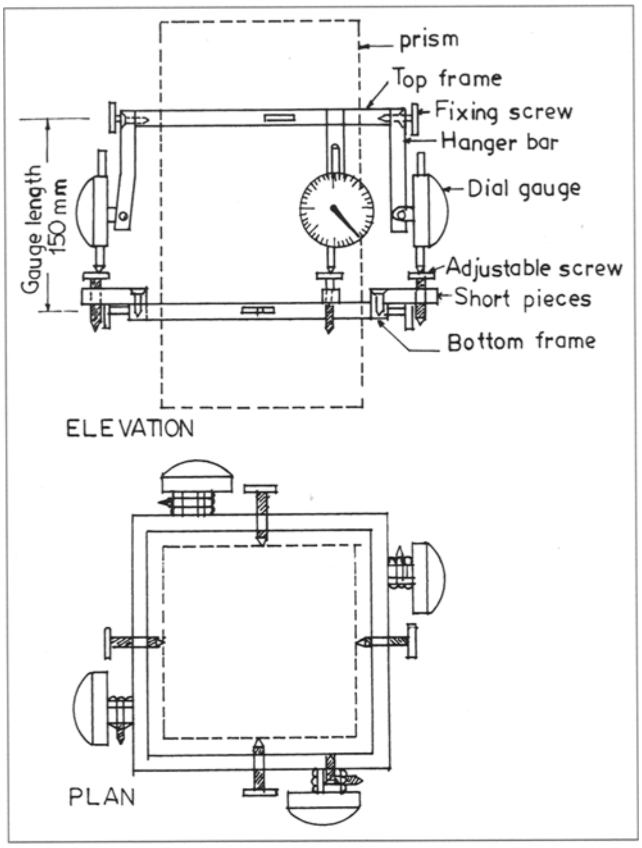

Fig. 2(a) – Details of compressometer.

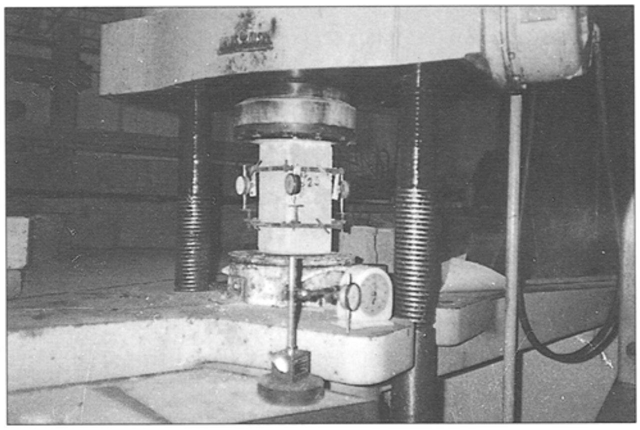

Fig. 2(b) – Compressometer attached to the prism.

screws at four points. The two frames were attached to the specimen symmetrically at the required gauge length, *i.e.* 150 mm apart. Two pairs of diametrically opposite dial gauges with a minimum count of 0.002 mm and a travel of 12 mm were attached to vertical hanger bars fixed to the top frame. The movable spindles of the dial gauges rested on the plane circular heads of the adjustable screws, which were positioned in mild steel plates projecting horizontally from the bottom frame. The frames were attached to the specimen by means of screws which would fit snugly to the concrete. Fig. 2(a) shows the details of the compressometer attached to the specimen. Fig. 2(b) shows the photograph of the same arrangement.

The capped specimen with the compressometer attached was placed on the movable cross head of the testing machine and tested under strain rate control. The

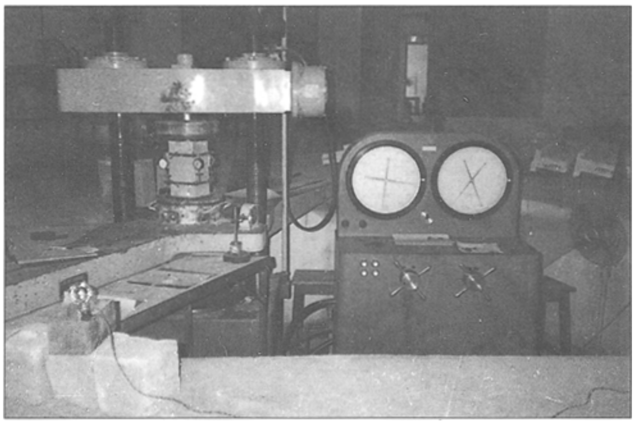

Fig. 3 - Testing of prism on 'TOTM'.

deformations were noted and strains were calculated. Fig. 3 shows the test arrangement. The test was continued until the load dropped to about 75 to 80 percent of the ultimate load in the post-ultimate region for both confined and unconfined concrete specimens.

3. INTERPRETATION AND DISCUSSION OF TEST RESULTS

3.1 Behaviour of test specimens under load

(A) General: The load increased rapidly in the initial stages up to about 75 percent of the peak load and thereafter increased at a slower rate until the peak load was reached. Tests were continued until the peak load dropped to about 0.75 to 0.80 times the peak load. Beyond the peak load, the strains increased at a rapid rate and were accompanied by a decrease in the load carrying capacity of the specimen.

(B) Reinforced Concrete (RC) Specimens: In the case of RC specimens, vertical cracks appeared in the cover region at about half of the peak load. As the load increased, the number of cracks increased and the width of cracks widened. The spalling of concrete cover was noticed before the peak load (*i.e.* at about 90 percent of peak load) was reached, but it was severe after passing the peak load.

(C) FCRC Specimens: In the case of FCRC specimens, fine vertical cracks appeared on the surface of the specimen at about 60 to 70 percent of the peak load. With the increase in load, the number of cracks increased and the width of cracks increased at a reduced rate compared to that of RC specimens. The behaviour of all the FCRC specimens up to 70 percent of the peak load of the confined RC specimens was about the same. Beyond the peak load, the mesh wires started bulging and the mortar cover over the mesh reinforcement started spalling. The extent of spalling became severe only after the load dropped to about 0.75 to 0.80 times the peak load. The extent of spalling and the rate of decrease of load after the peak (in the descending branch of the stress-strain curve) depended upon the specific surface factor (S_f) of the ferrocement shell if the tie confinement, as indicated by the confinement index, (C_i), was the same. The higher the specific surface factor (S_f), the lower the rate of decrease of load and the extent of spalling. This may be due to the improvement of the dimensional stability as well as the integrity of the material, caused by the presence of the large specific surface factor of the ferrocement shell provided as additional confinement to the core concrete. For some specimens with low values of specific surface factor ($S_f < 1.3$), it was observed that the peak loads were less compared to the peak loads observed in the corresponding RC specimens. However, in these specimens the extent of spalling of mortar cover after the peak load was found to be low compared to that in RC specimens. The maximum stress and strain at peak load and the strain at 85 percent of peak load in the descending portion of the stress-strain curve increased as the specific surface factor (S_f) increased with the same confinement index (C_i). The highest strain observed at maximum stress of any specimen was 0.035, and that at 0.85 times the maximum stress was 0.09 on the descending branch of the stress-strain curve, compared to 0.002 and 0.0035 for plain concrete specimens, respectively.

3.2 Experimental stress-strain curves

From the observed data, for a given specimen, the longitudinal deformations were calculated from the average readings of the four dial gauges of the compressometer. As there was no severe spalling in FCRC specimens until the load dropped by about 20 to 25 percent of peak load, the specimens were treated as dimensionally stable and hence the gross cross-sectional area was used in calculating the stress values. Stress-strain curves were drawn for the three companion specimens of a set with the same origin, and the average curve was taken to represent the set. Such average curves for all the sets of one typical batch with a common origin are shown in Fig. 4.

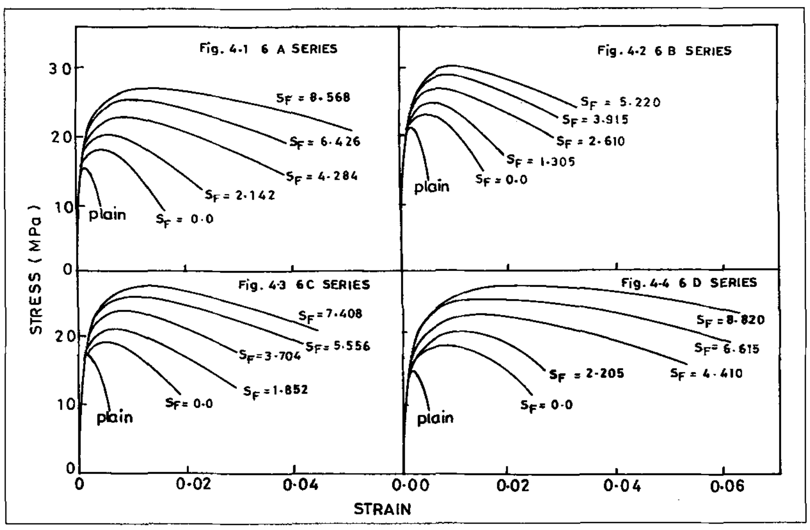

Fig. 4 - Stress-strain curves of 150 x 150 x 300 mm FCRC prisms.

3.3 Effect of specific surface factor on:

i) Ultimate strength: The ultimate strength of concrete increased with an increase in S_f for the same level of tie confinement. To quantify the effect of ferrocement shell confinement on ultimate strength, the effect of tie confinement is separated using the following equation:

$$f_{cb}\, Ag = K_t\, f'_c\, Ag \quad (1)$$

= the load taken by the tie confined concrete

where $K_t = 1 + 0.55\ C_i$ (2)

$$C_i = (P_b - P_{bb}) \times (f_y / f'_c) \sqrt{(b/s)} \quad (3)$$

Since the ultimate load carrying capacity (P) is experimentally determined, $(P - f_y\ A_s)$ gives the contribution to load carrying capacity due to both confinement of the ferrocement shell and tie confinement. This value is non-dimensionalised by dividing by $f_{cb}\ A_g$. This means that $K_f = (P - f_y\ A_s)/\ f_{cb}\ A_g$ gives the strength of concrete as a ratio of the strength of concrete confined by lateral ties only. A plot of K_f vs. S_f is given in Fig. 5. An examination of the plot shows that there is a linear relationship between K_f and S_f. A straight line is then fit between these two parameters. The linear equation thus obtained, with 90 percent confidence limits, is given below:

$$K_f = (0.9122 \pm 0.0054) + (0.0546 \pm 0.0012)\ S_f \quad \text{for } S_f \geq 1.6 \quad (4)$$

Therefore, it can be concluded that a low specific surface factor on the order of 1.6 does not have any beneficial effect on the strength of concrete. Hence, the final equation for the load carrying capacity (P) of concrete, confined with a ferrocement shell in addition to lateral ties, can be written as:

$$P = f'_c\,(1.0 + 0.55\ C_i)\,(0.912 + 0.055\ S_f)\ A_g + f_y\ A_s = f_{cf} A_g + f_y\ A_s \quad (5)$$

(ii) Strain at ultimate strength: The strain at ultimate strength increased with an increase in specific surface factor. Fig. 6 shows the plot between the ratio of observed strain (ε_{cf}) at the ultimate strength of concrete confined by a ferrocement shell, in addition to lateral ties, to the theoretical strain (ε_{cb}) at ultimate strength of concrete confined by lateral ties only and the specific surface factor (S_f). An examination of this plot clearly indicates that there is a linear relationship between S_f and the ratio of strain at the ultimate strength of concrete confined by a ferocement shell in addition to lateral ties to the strain of concrete confined by lateral ties only.

A straight line fit between the specific surface factor and the ratio $\varepsilon_{cf} / \varepsilon_{cb}$ resulted in the following equation:

$$\varepsilon_{cf} / \varepsilon_{cb} = (0.8939 \pm 0.0024) + (0.1776 \pm 0.0054)\ S_f \quad (6)$$

Hence, it can be concluded from the above equation that a low specific surface factor on the order of 0.56 cannot yield a beneficial effect on strains of concrete at ultimate stress.

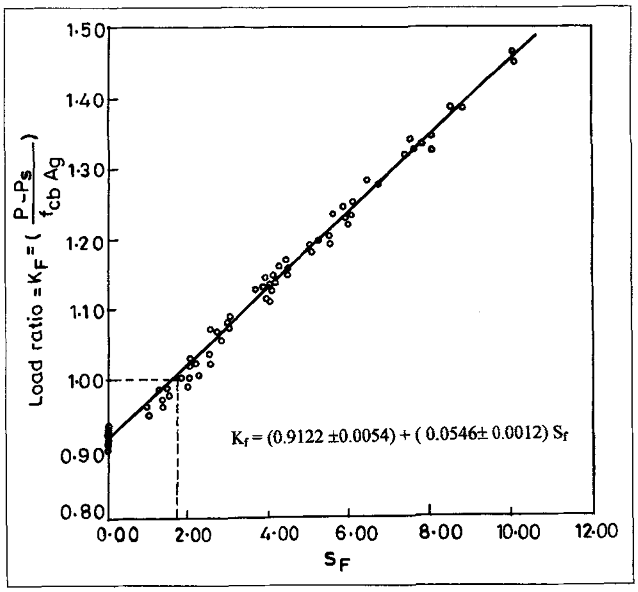

Fig. 5 – Load ratio (K_F) vs. specific surface factor (S_F).

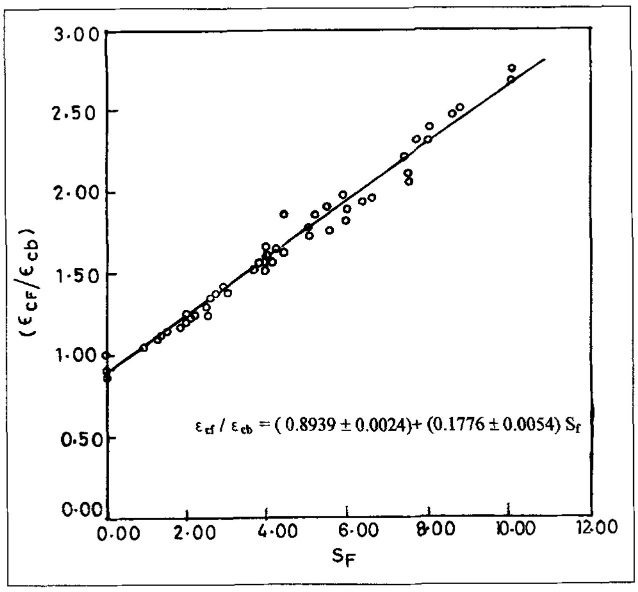

Fig. 6 – Ratio of strains at ultimate strength vs. specific surface factor.

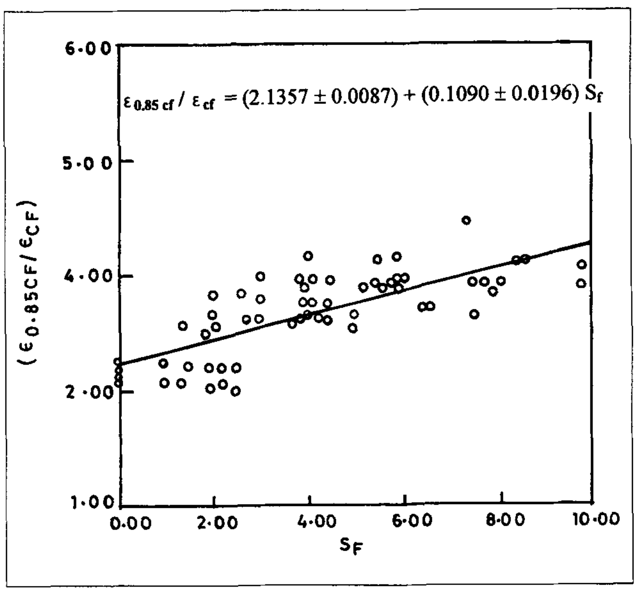

Fig. 7 – Ratio of strains at 0.85 of ultimate strength vs. specific surface factor.

The strain at ultimate strength of an FCRC section can be rewritten in the following form:

$$\varepsilon_{cf} = \varepsilon'_c (1.0 + 5.2\, C_i)(0.90 + 0.178\, S_f) \qquad (7)$$

(iii) Ductility of FCRC: The ductility of FCRC, as expressed by the strain at 85% of the ultimate strength in the descending portion of the stress-strain curve, is increased with an increase in the specific surface factor. The observed strain at 85 percent of the ultimate strength ($\varepsilon_{0.85\,cf}$) is expressed in terms of the theoretical strain (ε_{cf}) given by equation (7). A plot between the ratio $\varepsilon_{0.85\,cf}/\varepsilon_{cf}$ and the specific surface factor is given in Fig. 7. The following relationship is obtained between the above ratio and the specific surface factor.

$$\varepsilon_{0.85\,cf}/\varepsilon_{cf} = (2.1357 \pm 0.0087) + (0.1090 \pm 0.0196)\, S_f \approx 2.1 + 0.1\, S_f \qquad (8)$$

A glance at the test results showed that the influence of the specific surface factor is greater on the strain than on the strength. For a given value of specific surface factor ($S_f = 10$), the increase in strain at maximum stress is about 1.8 times the increase in strength, and the increase in strain at 85 percent of maximum stress is about 2.8 times the increase in strength of RC confined specimens. The effect of the ferrocement shell in confining the concrete is similar to that of transverse steel. Hence, the casting difficulties arising from situations of smaller spacing of transverse steel can be overcome to some extent by providing the ferrocement shell as additional confinement. Also, the ferrocement shell as additional confinement has the advantage, over confinement by lateral ties only, of improving material properties such as integrity, dimensional stability and performance under large deformations.

4. CONCLUSIONS

The following conclusions can be drawn from the experimental investigations on FCRC:

1. A ferrocement shell is an effective way of providing additional confinement of concrete in axial compression and has the advantage over lateral tie confinement of improving material performance under large deformations.

2. The additional confinement with the ferrocement shell improved the ultimate strength, the strain at ultimate strength and the ductility of concrete.

3. The improved ultimate strength with ferrocement shell confinement varied linearly with the specific surface factor, and can be expressed by a relationship which includes the two parameters C_i and S_f. The prediction equation for the ultimate load carrying capacity of an FCRC prism is:

$$P = f'_c (1.0 + 0.55\, C_i)(0.912 + 0.055\, S_f)\, A_g + f_y A_s \qquad (9)$$

4. The improved strain at ultimate strength with additional ferrocement shell confinement varied linearly with the specific surface factor and can be expressed as:

$$\varepsilon_{cf} = \varepsilon'_c (1.0 + 5.2\, C_i)(0.90 + 0.178\, S_f) \qquad (10)$$

REFERENCES

[1] Baker, A.L.L., 'The ultimate load theory applied to the design of reinforced and prestressed concrete frames' (Concrete Publications Ltd., London, 1956).

[2] Balaguru, P, 'Use of ferrocement for confinement of concrete', Proc. Third Int.Conf. on Ferrocement, Roorkee (India), 296-305.

[3] Ganesan, N. and Anil, J., 'Strength and behaviour of RC columns confined by ferrocement', *Jl of Ferrocement* **23** (2) 99-108.

[4] Paulay, T. and Priestley, M.J.N., 'Seismic design of reinforced concrete and masonry buildings' (John Wiley and Sons, New York, 1992).

[5] Rao, A.K., Reddy, K.N. and Reddy, V.M., 'Effect of stirrup confinement on flexural behaviour of prestressed concrete simple beams ', *Journal of IE (India)* **59** Part-I 258-266.

[6] Rao, C.B.K. and Rao, A.K., 'Stress strain curve in axial compression and Poisson's ratio of ferrocement', *Jl. of Ferrocement* **16** (2) 117-128.

[7] Reddy, S.R., 'Behaviour of concrete confined in rectangular binders and its application in flexure of reinforced concrete structures', Thesis submitted to J.T. University, Hyderabad (India), for Ph.D Degree, February 1974.

[8] Seshu, D.R., 'Behaviour of concrete confined with ferrocement shell in addition to rectangular stirrups and its application in flexure of RC structures', Ph.D Thesis submitted to Kakatiya University, Warangal (India) 1995.

[9] Sheikh, S.A., 'Comparative study of confinement models', *Journal of ACI* **79** (4) 296-306.

[10] Waliudin, A.M. and Rafeeqi, S.F.A., 'Study of behaviour of plain concrete confined with ferrocement', *Jl of Ferrocement* **24** (2) 139-145.